Fundamental, Binary Combination, and Overtone Modes in Methoxy Adsorbed on Cu(100): Infrared Spectroscopy and Ab Initio Calculations

M. P. Andersson and P. Uvdal*

Chemical Physics, Department of Chemistry, Lund University, PO Box 124, S-221 00 Lund, Sweden

A. D. MacKerell, Jr.

Department of Pharmaceutical Sciences, School of Pharmacy, University of Maryland at Baltimore, Baltimore, Maryland 21201

Received: July 31, 2001; In Final Form: March 6, 2002

Using surface infrared absorption spectroscopy, we have measured and assigned the vibrational spectra of six different methoxy isotopomers adsorbed on a Cu(100) surface in great detail. The assignments are based on ab initio calculations of the vibrational mode frequencies of all six isotopomers for a methoxy−Cu_5 complex. By combining different IR detectors and optical filters, we observe many, previously undetected, weak spectral features, which we can assign as various binary overtone and combination modes. On the basis of these binary modes conclusions on the intramolecular anharmonic coupling in the adsorbate can be drawn.

1. Introduction

For a long time, vibrational studies of alkoxies adsorbed on single-crystal metal surfaces have served as model systems for adsorption of organic molecules containing a functional group. It is well-documented that a stable alkoxy species is formed on the surface either upon adsorption or through reaction with preadsorbed atomic oxygen. In particular, one is interested in how the coordination of the oxygen to the metal surface is reflected in the carbon skeleton and carbon hydrogen modes. A correct interpretation and assignment of the vibrational modes is desirable as it, for example, means that the symmetry of the adsorbate can be determined. From the symmetry, information about the adsorbate geometry can be obtained. The interpretation and assignment of the vibrational spectrum of even such a simple adsorbate as methoxy have, however, been the source of some controversies over the years in the surface science literature. Because methoxy contains only nine intramolecular fundamental modes in three well-separated regions of the spectrum, it would seem like a straightforward thing to assign its vibrational modes. In addition by applying symmetry rules and the surface dipole selection rule, the number of dipole-allowed modes may be further reduced. In the specific case of methoxy, the presence of a mirror plane will reduce the number of dipole-allowed fundamental modes to six or less, depending on the orientation of the modes within the plane. For instance, the number of dipole-allowed fundamental C−H stretch modes will be one or two, depending on the orientation of the C−O axis within the plane. For a C_{3v} symmetric species, that is, C−O axis perpendicular to the surface, the number of dipole-allowed fundamental modes will be reduced to 3, see Table 1. The number of dipole-allowed fundamental C−H stretch modes will be reduced to a single mode. The experimentally observed vibrational spectrum of methoxy exhibits three modes in the C−H stretch region, 2700−3100 cm^{-1}, for most metal surfaces, Cu(100),[1] Cu(110),[2] Cu(111),[3] Mo(110),[4] Ni(110),[5] Ni(100),[6] and W(110).[7] From a first-order analysis, it therefore appears as methoxy adsorbed on these metal surfaces has lost all symmetry elements and therefore is oriented with the C−O axis in some tilted fashion with respect to the surfaces normal, which also breaks the mirror plane of methoxy. Using this first-order analysis, Ryberg[1] concluded that methoxy is tilted on Cu(100). It was, however, apparent already in this work that there was some problems with the first-order interpretation. The observed intensity relation between the three C−H stretch modes was different from the intensity relation between the C−D stretch modes in deuterated methoxy. Later, Chesters and McCash[3] correctly assigned the three modes of methoxy on Cu(111) to one fundamental ($\nu_s(CH_3)$) and two overtones from the fundamental ($\delta_s(CH_3)$ and $\delta_{as}(CH_3)$) modes in Fermi resonance (FR) with the fundamental mode. The assignment was based on a comparison with an osmium cluster and the above-mentioned intensity redistribution of the methyl stretches upon deuteration. The problem with this assignment was that it is consistent with both C_s and C_{3v} symmetry of the adsorbate and that this Fermi resonance explains the intensity redistribution upon deuteration but the resonance should appear for both symmetries. The main controversy in the following is the assignment of the IR band with the highest frequency, <2900 cm^{-1}, of the three bands

TABLE 1: Irreducible Representation of Methoxy Modes in the Possible Point Group Symmetries C_{3v}, C_s and C_1[a]

mode	C_{3v}	C_s	C_1	experimentally observed
ν(CO)	**A_1**	**A′**	**A**	yes
$\rho(CH_3)$	E	**A′**	**A**	
$\rho(CH_3)'$	E	A″	**A**	
$\delta_s(CH_3)$	**A_1**	**A′**	**A**	yes
$\delta_{as}(CH_3)$	E	**A′**	**A**	
$\delta_{as}(CH_3)'$	E	A″	**A**	
$\delta_s(CH_3)$	**A_1**	**A′**	**A**	yes
$\delta_{as}(CH_3)$	E	**A′**	**A**	
$\delta_{as}(CH_3)'$	E	A″	**A**	

[a] Observable modes in reflection/absorption infrared spectroscopy are marked in bold.

* To whom correspondence should be addressed. E-mail: per.uvdal@chemphys.lu.se.

10.1021/jp012939s CCC: $22.00
Published on Web 05/01/2002

observed in the C−H stretch region. As above, the band has alternatively been assigned to the fundamental $\nu_{as}(CH_3)$ mode[1,8,9] or the overtone $2 \times \delta_{as}(CH_3)$ mode[3]. The difficulties involved in using metal clusters for assignments of surface adsorbates are illustrated by the work by U. A. Jayasooriya et al.[10] and Dastoor, Gardner and King.[8] Two different Re clusters with methoxy coordinated to two or three metal atoms were studies by U. A. Jayasooriya et al.. On the basis of an erroneous assignment of the C−H stretch mode in question to the fundamental $\nu_{as}(CH_3)$, they concluded that methoxy in general is tilted on most metal surfaces.[10] These results were used by Dastoor, Gardner, and King to assign the mode for methoxy adsorbed on Ni(110) as a fundamental mode. The assignment was also based on the observation of both the $\rho(CH_3)$ and $\delta_{as}(CH_3)$ modes, which showed that the methoxy is tilted on Ni(110). The same assignment was likewise used by Zenobi et al. for methoxy on Ni(111).[9] The controversy was finally solved by Uvdal, Weldon, and Friend.[4] Using CHD_2O- adsorbed on Mo(110), they demonstrated that the C−O axis is oriented along the surface normal because only a single C−H stretch mode is observed. For a tilted species, two modes should be present arising from the two rotational conformers possible, C−H bond in or out of the molecular plane. The nonlabeled species, however, exhibited three C−H stretch modes on Mo(110) in accordance with what is observed on most metal surfaces. The mode at ∼2900 cm^{-1} could then conclusively be assigned as the $2 \times \delta_{as}(CH_3)$ mode. This assignment has later been used by Sim, Gardner, and King for methoxy adsorbed on Ag(111),[2] by Huberty and Madix for Ni(100),[6] and by Camplin and McCash[11] and Mudalige et al.[12,13] for Cu(100). A qualitative analysis of the Fermi resonances between the fundamental $\nu_s(CH_3)$ mode and the $2 \times \delta_s(CH_3)$ and $2 \times \delta_{as}(CH_3)$ overtone modes in methoxy on Cu(100) has also been given by Ásmundsson and Uvdal.[14]

To conclude, it is instructive to see that even an apparently simple system has led to many conflicting assignments before a consensus finally was reached. It is also interesting to notice that the pronounced influence from Fermi resonance coupling between the $\nu_s(CH_3)$ mode and the overtones from the $\delta(CH_3)$ modes in a methyl group was quite well-understood already in the seventies for, for example, methylhalides.[15] The reason for the controversy in the surface science community almost twenty years later was mostly a result of poor communication with or poor knowledge about results produced by spectroscopists studying small molecules in noble gas matrixes.

In the present work, we make a detailed study of methoxy adsorbed on Cu(100) using an optimized optical set up for surface studies, which includes the use of filters. A complete and conclusive assignment of the vibrational spectra of five different methoxy isotopomers is made, including several overtone and combination modes. The assignment is accomplished with the aid of ab initio electronic structure calculations using a CH_3O-Cu_5 cluster to model the surface adsorbate. The vibrational spectra of all of the investigated isotopomers, ^{13}C and deuterium, were also calculated. Our highly sensitive spectrometer allows us to detect and assign several previously unobserved or unassigned absorption lines for methoxy adsorbed on Cu(100). In a recent feature article, M. Trenary and co-workers[12] detected and assigned 25 absorption lines for the same set of isotopomers as studied here on Cu(100). We detect and assign an additional seven lines in the present work. We also show that these lines are due to binary modes and that our calculations are necessary for the assignment of them. This is because many of the fundamental modes constituting the binary modes are not experimentally accessible, either because of not being totally symmetric or because of their weak intensity.

2. Experimental Section

Experiments were conducted using a Bruker IFS 66v/S FTIR spectrometer connected to a UHV chamber (base pressure 7×10^{-11} Torr) in which the Cu(100) sample was mounted. The crystal was oriented with an accuracy of <0.5° and was cleaned by 500 eV argon ion sputtering and annealing cycles to 600 K. Occasional oxygen treatments (500 L of O_2 at 600 K) were done before the sputter−anneal cycles to keep the carbon contamination of the surface low. The surface cleanliness was monitored by Auger electron spectroscopy, and the surface was judged clean when only trace amounts of carbon were detected. High reproducibility of the spectra over several months further confirmed the surface purity. The adsorbate layer was prepared by dosing 2 L of oxygen onto the clean surface at 470 K, followed by dosing the oxygen-covered surface with 3 L of methanol at ∼85 K and annealing the surface to 350 K for 30 s. This procedure gives a methoxy coverage of about 0.3 ML judging from the position of the CO stretch.[16] Methanol was purchased from Aldrich (spectroscopic grade), and all other isotopomers were purchased from Cambridge Isotope Laboratories (atom purities: ^{13}C 99%, D 98%, D_2 98%, D_3 99% and $^{13}CD_3$; ^{13}C 99% and D_3 99%). All were further purified by several freeze−pump−thaw cycles before being let into the UHV chamber. The spectrometer resolution was 0.5 cm^{-1} unless otherwise stated, and a boxcar apodization function was used. All spectra in the region 600−1700 cm^{-1} were recorded with an MCT detector with a low-pass filter (6000 nm, Spectrogon), and all spectra in the region 1850−3200 cm^{-1} were recorded with an InSb detector with a low-pass filter (3000 nm, Spectrogon). All spectra were recorded at <90 K, and the total sample scan time was 30−40 min. Occasional 350 K flashes were done to reduce the effect of readsorption of methanol or adsorption of other contaminants. Backgrounds both before methanol dosing and after a 560 K flash were used. Baseline correction has been made on all spectra in the high-frequency region (1800−3300 cm^{-1}) by subtracting a straight line from the original spectrum.

3. Calculations

The ab initio electronic structure calculations were performed with a Gaussian 98 package[17] using the HF/LanL2DZ model chemistry. We have previously used a single metal atom to represent the surface[18] but will here use a more realistic model. A five copper atom cluster for which all degrees of freedom were frozen represented the Cu(100) surface. Four atoms in a square represented the top layer, and the fifth atom placed in the hollow site represented the second layer. The interatomic distances were chosen to be those of bulk fcc copper, that is, a nearest neighbor distance of 2.556 Å. The methoxy molecule was then placed with its oxygen toward the surface in the 4-fold hollow site of the cluster as experiments indicate hollow adsorption on Cu(111).[19] In addition, to further explore the adsorption site, calculations of methoxy on a Cu_8 cluster were made, Figure 1, where the methoxy species was positioned in the bridge site when the optimization was started. Upon optimization, the methoxy species moved from the bridge position to the hollow site. For this optimized geometry, all intramolecular modes differed less than 16 cm^{-1} from the ones presented in this paper, showing that the intramolecular modes have already converged for a five-atom copper cluster. The

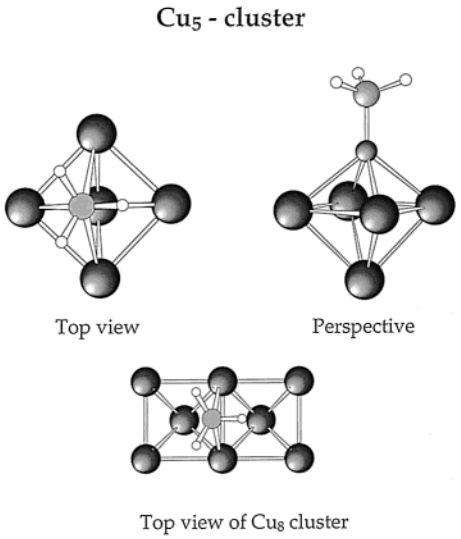

Figure 1. Cluster models used in the calculations.

methoxy−Cu_8 cluster exhibits C_{2v} symmetry in contrast to the higher C_{4v} symmetry of the hollow site on the surface. This introduces an unphysical asymmetry in the surface−adsorbate interaction, which is hard to estimate. Lower symmetry results in an increased coupling between modes. In this particular case, this gives more coupling between the frustrated adsorbate modes and the metal cluster modes. As a result, the frustrated modes are probably better modeled by the methoxy−Cu_5 cluster than by the methoxy−Cu_8 cluster for symmetry reasons alone. The coupling is indeed much more complicated for the methoxy−Cu_8 cluster, and the six frustrated modes are not so easily identified as those for the methoxy−Cu_5 cluster. In addition, the smaller cluster is also computationally less expensive, and we have therefore used the methoxy−Cu_5 cluster to calculate the intramolecular modes presented here. Because the focus of the paper is on the intramolecular modes the choice of cluster is less important. Geometry optimization of the methoxy−Cu_5 cluster was performed with enforced C_s symmetry due to the unphysical optimized structure obtained when all symmetry constraints were lifted. The optimized geometry is shown in Figure 1. Wave function stability calculations were also made to ensure that the geometry optimization and frequency calculations were performed for the electronic ground state (in this case a triplet state). Finally, the adsorption site was also investigated by calculations for on-top geometry (using one Cu atom) and bridge geometry (using two copper atoms).[20] Both complexes give higher values for the CO stretch mode (1149 cm^{-1} for the on-top and 1064 cm^{-1} for the bridge) than the Cu_5 cluster at 1006 cm^{-1}, which agrees with the experimental result, 998 cm^{-1}. These observations are also consistent with an adsorption in the 4-fold hollow site.

As in previous publications[18,14] calculated vibrational frequencies were scaled by 0.9 to account for electron correlation neglected by using the HF method. We have found no calibration of the scaling factor for the HF/LanL2DZ model chemistry in the literature, and therefore, we use our previous scale factor. This has worked well before and also enables us to make comparisons with previous calculations. The calculated vibrational frequencies are summarized in Tables 2−5 and the vibrations are given symmetry within the calculated C_s point group found for the optimized geometry. In addition, for the CH_3O− and CD_3O− species that exhibit an effective C_{3v} symmetry, intramolecular modes that are degenerate within C_{3v} symmetry are next to one another in the table and are marked with an E in parentheses. MOLVIB[21] was used to analyze the internal methoxy vibrations for all isotopomers, and the potential energy distribution of the modes are included in Figures 2−5 along with the frequencies. The substrate modes and the frustrated rotational and translational modes, however, were not analyzed this way because of the difficulty in setting up modes giving intuitive results and easily presentable data. For these modes, GAUSSVIEW was used to analyze the results. The program allows for animation of the calculated vibrational modes, which permits a "visual" identification of the frustrated degrees of freedom. Frustrated modes should, furthermore, exhibit a considerably lower reduced mass than the substrate modes (if uncoupled). Finally, isotopic shift induced by both D_3 and ^{13}C were used, expecting a larger shift for the frustrated modes than substrate modes, which if uncoupled would not shift at all. The isotopic shifts and the reduced masses of the nine cluster modes and the six frustrated modes are shown in Table 6. From these data, five of the frustrated modes are easily sorted out: 3, 4, 9, 13, and 15. These five modes have the lowest reduced masses and at the same time the highest H_3 to D_3 shifts. Furthermore, the ^{13}C shifts are entirely consistent with this assignment as well. Note that the torsion about the CO axis is virtually unshifted (the carbon atom is stationary) whereas the other four modes show the highest shifts. Identifying the last frustrated mode is slightly more difficult, because by comparison of the reduced masses and H_3 to D_3 shifts modes 1 and 11 are very similar. The ^{13}C shift, however, is larger for mode 1, and from the mode animation in GAUSSVIEW assignment of FT_{xy} to mode 1 is a better choice. All six frustrated modes identified in this manner are included in Tables 2−5. The frustrated translation of A″ symmetry parallel to the surface, mode 1, has an imaginary frequency, which probably arises from the enforced C_s symmetry of the cluster. In addition, the fact that there is a cluster mode, mode 11, with a reduced mass as low as the FT_{xy} mode indicates that there is strong coupling between the cluster modes and the frustrated modes. This could be another explanation of the imaginary frequency for the FT_{xy} mode.

A restrained geometry like this will generally give rise to imaginary frequencies because of the fact that the system along the frozen coordinates is not on a stationary point on the potential energy surface (in the subspace without the frozen coordinates, however, it is.). It is therefore important to be able to distinguish between an imaginary frequency arising from being on a maximum along a normal coordinate and an imaginary frequency arising from a frozen coordinate. We have performed frequency calculations on the bare Cu_5^{+1} cluster and found that it has one imaginary frequency, that is, the methoxy−Cu_5 cluster has one more imaginary frequency. If the symmetry constraints are lifted, the geometry optimization gives an unphysical structure. The good agreement between experimental and calculated frequencies and the low value of the imaginary frequency make us confident that our methoxy−Cu_5 complex represents the present adsorbate−surface system well.

4. Experimental Results

4.1. Overview Spectra, Figures 2 and 3. An overview of the infrared absorption spectra for all isotopomers is shown in Figures 2 and 3. Only the frequencies of modes with a peak height of >0.1% are shown. In Figure 2, all observed modes are fundamentals, whereas only a fraction of the observed modes in Figure 3 are fundamentals. The assignment of the fundamental modes is summarized in Table 2−5 along with the calculated values. The agreement between calculations and experiments

TABLE 2: Experimental and Calculated Fundamental Frequencies and Isotopic ^{12}C to ^{13}C Shifts for $^{12}CH_3O-Cu(100)$

mode number	symmetry	exptl frequency (cm^{-1})	calcd frequency (cm^{-1})	calcd isotopic shift (cm^{-1})	calcd intensity (a.u.)	modes and potential energy distribution (%)			
1	A″		−104	0.5	13	FT_{xy}			
2	A′		−80	0.2	2				
3	A″		57	0.0	0	$\tau(OCH_3)$			
4	A′		71	−0.8	5	FT_{xy}			
5	A″		83	−0.1	0				
6	A″		87	0.0	1				
7	A′		93	−0.3	3				
8	A′		112	−0.3	4				
9	A″		125	−1.4	3	FR			
10	A′		132	−0.3	0				
11	A″		132	−0.2	5				
12	A″		136	0.0	1				
13	A′		154	−1.3	25	FR			
14	A′		174	0.0	1				
15	A′	304[a]	271	−2.4	22	FT_z			
16	A′	998	1006	−18.2	272	ν(C−O)	100		
17	A″ (E)		1124	−7.6	0	$\rho(CH_3)'$	96		
18	A′ (E)		1128	−7.6	2	$\rho(CH_3)$	96		
19	A′	1426	1446	−5.9	22	$\delta_s(CH_3)$	103		
20	A″ (E)		1488	−3.0	2	$\delta_{as}(CH_3)$	73	$\delta_{as}(CH_3)'$	24
21	A′ (E)		1488	−2.9	4	$\delta_{as}(CH_3)'$	73	$\delta_{as}(CH_3)$	24
22	A′	2808[b]	2836	−2.4	206	$\nu_s(CH_3)$	100		
23	A″ (E)		2894	−10.5	47	$\nu_{as}(CH_3)$	100		
24	A′ (E)		2901	−10.5	44	$\nu_{as}(CH_3)'$	100		

[a] Reference 30. [b] In heavy Fermi resonance with the bend overtones (ref 13).

TABLE 3: Experimental and Calculated Fundamental Frequencies for $^{12}CH_2DO-Cu(100)$ in C_s Symmetry (*D* in mirror plane)

mode number	symmetry	exptl frequency (cm^{-1})	calcd frequency (cm^{-1})	calcd intensity (a.u.)	calcd isotopic shift (cm^{-1})	modes and potential energy distribution (%)	
1	A″		−103	13	0.4	FT_{xy}	
2	A′		−80	2	0.1		
3	A″		50	0	0.0	$\tau(OCDH_2)$	
4	A′		69	4	−0.8	FT_{xy}	
5	A′		83	0	0.0		
6	A″		87	1	0.0		
7	A′		92	3	−0.2		
8	A′		111	3	−0.2		
9	A′		122	4	−1.5	FR	
10	A″		131	4	−0.1		
11	A′		132	0	−0.2		
12	A″		136	1	0.0		
13	A′		151	26	−1.1	FR	
14	A′		174	1	−0.1		
15	A′		264	21	−2.3	FT_z	
16	A′	922	907	9	−4.9	δ(OCD)	90
17	A′	1006	1007	260	−18.7	ν(C−O)	91
18	A″		1091	0	−10.4	$\rho(CH_2)$	89
19	A″		1296	2	−0.9	$tw(CH_2)$	89
20	A′		1350	18	−6.9	$w(CH_2)$	101
21	A′		1478	6	−3.5	$sc(CH_2)$	102
22	A′	2144	2112	54	−11.3	ν(CD)	99
23	A′	2913	2856	166	−5.6	$\nu_s(CH_2)$	100
24	A″		2894	46	−10.7	$\nu_{as}(CH_2)$	99

for the fundamentals is excellent with an error no greater than 2.2% and allows for a conclusive assignment of the fundamental modes. Where strong Fermi resonances are involved, the fundamental is assigned as the mode with the highest intensity, even though the states are heavily mixed.

In Figure 2a,a′, an intense single line is observed at 998 and 977 cm^{-1}, respectively. It is assigned to the ν(C−O) mode (Table 2). The isotopic shift of 21 cm^{-1} is in agreement with the calculated, 18.2 cm^{-1}. The additional modes observed for $^{13}CH_3O-$, Figure 2a′, can all be attributed to isotopic contamination. The small mode at 986 cm^{-1} for $^{13}CH_3O-$ is assigned as the (singleton) ν(C−O) mode for the $^{12}CH_3O-$ species (<1% abundance). Its intensity is probably enhanced through dynamic dipole coupling. The weak feature at 939 cm^{-1} is the ν(C−O) mode of $^{13}CH_3{}^{18}O-$, Figure 2a′. ^{13}C-labeled compounds typically contain higher amounts of ^{18}O than nonlabeled ones, sometimes as high as 10−20%, although normally less.[22] Our calculations determined the isotopic shift between $^{13}CH_3{}^{18}O-$ and $^{12}CH_3{}^{16}O-$ to be ∼50 cm^{-1}, which is in agreement with the experimental shift of 47 cm^{-1}. The assumption is made that the dipole shift of the C−O stretch for both $^{12}CH_3{}^{16}O-$ and $^{13}CH_3{}^{18}O-$ was negligible.

The partially deuterated species CH_2DO- and CHD_2O-, Figure 2b,c, are also straightforward to assign based on the calculations, Tables 3 and 4. The absorption lines at 922 (Figure 2b) and 949 cm^{-1} (Figure 2c) are assigned to the δ(OCD) mode

TABLE 4: Experimental and Calculated Fundamental Frequencies for $^{12}CHD_2O-Cu(100)$ in C_s Symmetry (H in mirror plane)

mode number	symmetry	exptl frequency (cm^{-1})	calcd frequency (cm^{-1})	calcd isotopic shift (cm^{-1})	calcd intensity (a.u.)	modes and potential energy distribution (%)					
1	A″		−103	0.5	13	FT_{xy}					
2	A′		−80	0.2	2						
3	A″		44	0.0	0	$\tau(OCD_2H)$					
4	A′		68	−0.7	4	FT_{xy}					
5	A′		83	0.0	0						
6	A″		87	0.0	1						
7	A′		92	−0.2	3						
8	A′		111	−0.2	3						
9	A″		116	−1.3	5	FR					
10	A″		130	0.0	3						
11	A′		131	0.0	0						
12	A″		136	0.0	1						
13	A′		146	−0.9	24	FR					
14	A′		174	−0.1	1						
15	A′		268	−2.3	20	FT_z					
16	A″		868	−5.5	0	$tw(CD_2)$	52	$\rho(CD_2)$	46		
17	A′	949	929	−5.5	61	$w(CD_2)$	39	$\nu(CO)$	36	$\delta(OCH)$	22
18	A′	1007	1019	−18.6	189	$\nu(CO)$	61	$w(CD_2)$	24		
19	A′	1067	1088	−7.5	25	$sc(CD_2)$	99				
20	A′		1321	−4.0	16	$\delta(OCH)$	66	$w(CD_2)$	37		
21	A″		1333	−4.2	1	$\rho(CD_2)$	53	$tw(CD_2)$	48		
22	A′	2099	2067	−7.5	113	$\nu_s(CD_2)$	100				
23	A″		2147	−15.4	25	$\nu_{as}(CD_2)$	100				
24	A′	2905	2884	−8.4	72	$\nu(CH)$	100				

TABLE 5: Experimental and Calculated Fundamental Frequencies for $^{12}CD_3O-Cu(100)$

mode number	symmetry	exptl frequency (cm^{-1})	calcd frequency (cm^{-1})	exptl isotopic shift (cm^{-1})	calcd isotopic shift (cm^{-1})	calcd intensity (a.u.)	modes and potential energy distribution (%)				
1	A″		−103		0.6	13	FT_{xy}				
2	A′		−80		0.1	2					
3	A″		41		0.0	0	$\tau(OCD_3)$				
4	A′		67		−0.8	4	FT_{xy}				
5	A′		83		0.0	0					
6	A″		87		0.0	1					
7	A′		91		−0.1	3					
8	A′		111		−0.2	3					
9	A″		112		−1.1	6	FR				
10	A″		130		0.0	3					
11	A′		131		−0.1	0					
12	A″		136		0.0	1					
13	A′		144		−0.7	25	FR				
14	A′		174		−0.1	1					
15	A′		262		−2.1	19	FT_z				
16	A″ (E)		867		−6.1	0	$\rho(CD_3)'$	98			
17	A′ (E)		870		−6.1	1	$\rho(CD_3)$	98			
18	A′	971	970	−9	−7.5	191	$\nu(C-O)$	87			
19	A″ (E)		1081		−4.5	2	$\delta_{as}(CD_3)$	74	$\delta_{as}(CD_3)'$	25	
20	A′ (E)		1081		−4.6	1	$\delta_{as}(CD_3)'$	75	$\delta_{as}(CD_3)$	25	
21	A′	1086	1104	−13	−16.5	90	$\delta_s(CD_3)$	91			
22	A′	2053	2031	−6	−4.1	132	$\nu_s(CD_3)$	100			
23	A″ (E)		2146		−15.5	25	$\nu_{as}(CD_3)$	99			
24	A′ (E)		2151		−15.6	24	$\nu_{as}(CD_3)'$	99			

and $w(CD_2)$ mode, respectively. The lines at 1006 and 1007 cm^{-1} are assigned to the $\nu(C-O)$ modes. Finally, the assignment of the line at 1067 cm^{-1} in Figure 2c to the $sc(CD_2)$ mode also follows from the calculations.

The CD_3O- and $^{13}CD_3O-$ species, Figure 2d,e, are analogous to the nondeuterated species. The calculated values are shown in Table 5. Once more, the absolute values together with the isotopic shifts allow for a conclusive assignment of the observed modes. The band at 971 and 962 cm^{-1} is assigned as the $\nu(C-O)$ mode, and the lines at 1085 and 1072 cm^{-1} are assigned as the $\delta_s(CD_3)$ mode. As for the $^{13}CH_3O-$ species, isotopic contamination gives a contribution in the $^{13}CD_3O-$ spectrum; the line 922 cm^{-1} for $^{13}CD_3O-$ is the CO stretch of $^{13}CD_3{}^{18}O-$.

An overview of the most intense modes in the C−D and C−H stretch region is shown in Figure 3a−e. In contrast to the 600−1600 cm^{-1} region, the spectra in the 1800−3200 cm^{-1} region cannot be assigned to fundamentals only. A pronounced mixing of overtones with fundamentals is observed. Fermi resonances in the C−H and C−D stretch region for CH_3O- and CD_3O- adsorbed on metal surfaces are well-known and have been reported previously.[3,4,14] In short, the symmetric C−H or C−D stretch is coupled through anharmonicity to the overtones of the symmetric and asymmetric bend modes to give three peaks in the C−H or C−D stretch region. The coupling is stronger to the overtone of the symmetric bend than to the overtone of the asymmetric bend, which has been shown for CH_3O- on various metals both experimentally[14] and theoretically.[23] The assignment of the CH_3O- spectrum in Figure 3a follows the assignment made in ref 14, for details see Tables 2 and 7.

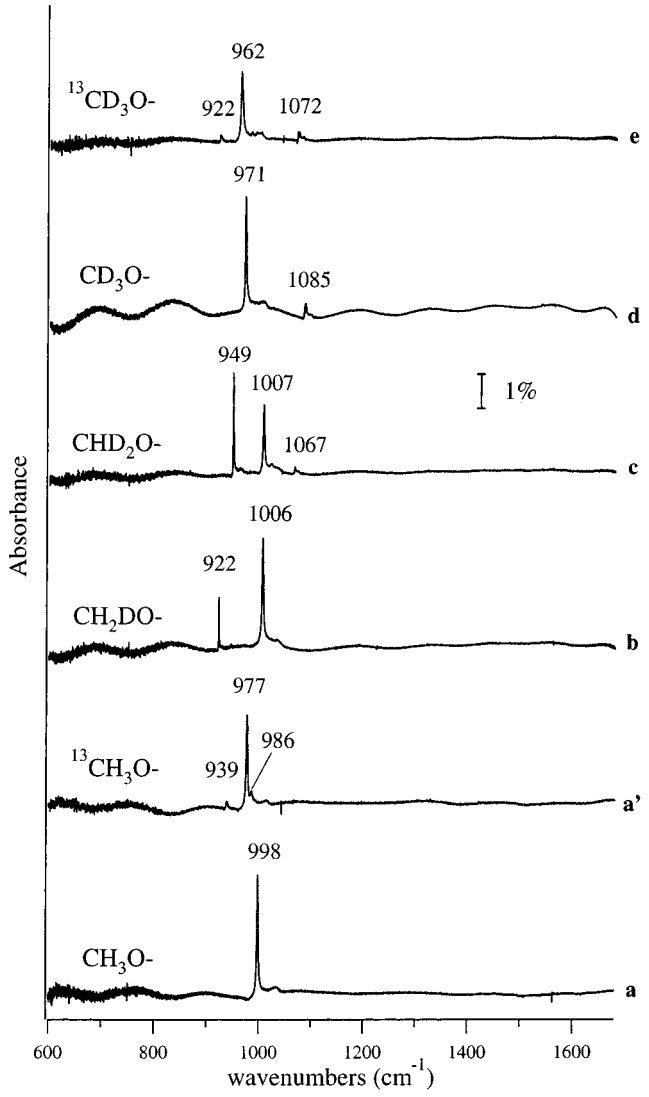

Figure 2. Infrared absorption spectra of (a) CH_3O-, (a′) $^{13}CH_3O-$, (b) CHD_2O-, (c) CH_2DO-, (d) CD_3O-, and (e) $^{13}CD_3O-$ adsorbed on Cu(100).

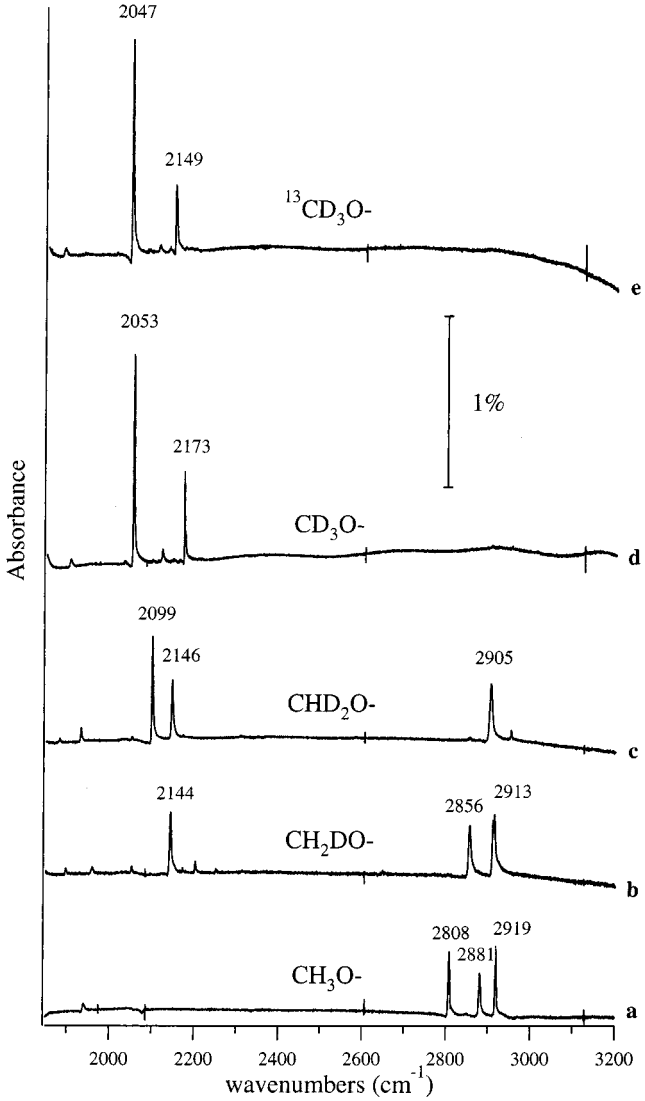

Figure 3. Infrared absorption spectra of (a) CH_3O-, (b) CHD_2O-, (c) CH_2DO-, (d) CD_3O-, and (e) $^{13}CD_3O-$ adsorbed on Cu(100).

The two partially deuterated isotopomers exhibit, as expected, some clear similarities. The lines at 2144 and 2913 cm^{-1} in CH_2DO- are assigned as two fundamentals, ν(C−D) and $\nu_s(CH_2)$, respectively, in agreement with calculations, Table 3. Accordingly, the lines at 2099 and 2905 cm^{-1} in CHD_2O- are assigned to the fundamental $\nu_s(CD_2)$ and ν(C−H) modes, respectively, see Table 4. The intense lines at 2856 cm^{-1} for CH_2DO- and 2146 cm^{-1} for CHD_2O- are assigned as the overtones of the symmetric bend modes, that is, $2 \times sc(CH_2)$ and $2 \times sc(CD_2)$, respectively, their high-intensity being due to Fermi resonances. As a result, the $2 \times sc(CH_2)$ mode is shifted down (∼100 cm^{-1}) as compared to the calculated value for the fundamental. The downshift is attributed to both anharmonicity and FR repulsion from the fundamental $\nu_s(CH_2)$ mode. The $2 \times sc(CD_2)$ mode shifts up (12 cm^{-1}), based on the experimental value (2×1067 $cm^{-1} = 2134$ cm^{-1}) of the fundamental, Table 7. This is again consistent with FR repulsion from the fundamental $\nu_s(CD_2)$ mode. Based on the calculated frequencies only, the assignment in the modes at 2856 and 2913 cm^{-1} CH stretch region of CH_2DO- would be reversed. This is, however, a two-state Fermi resonance with all of the intensity coming from the fundamental. As a consequence, the mode with the highest intensity has to have the highest component of fundamental mode, and hence, the most intense mode (2913 cm^{-1}) is assigned as $\nu_s(CH_2)$.

The assignment of the observed lines of CD_3O- and $^{13}CD_3O-$ species in this frequency region is analogous to the nondeuterated species, for assignments see Tables 5 and 7. The most striking difference is the much lower intensity of the $2 \times \delta_{as}(CD_3)$ mode, at 2122 cm^{-1}, as compared to the $2 \times \delta_{as}(CH_3)$ mode, at 2919 cm^{-1}, of the nondeuterated species in relation to the fundamental C−D and C−H stretch. Also note that the order of the modes is reversed (i.e., the frequency of the symmetric bend overtone is higher than the overtone of the asymmetric bend) for CD_3O-, which follows from the changed order of the fundamentals, compare Tables 2 and 5.

To conclude, there is a clear analogy between the two partially deuterated C_s species and the nondeuterated and fully deuterated C_{3v} species in that the symmetric stretch of the majority isotope, H or D, is in strong Fermi resonance with the overtone of the symmetric bend of the same atoms. The splitting of the mode at 2913 cm^{-1} for CH_2DO- seems to be a coverage effect. The splitting vanishes for both lower and higher coverages (not shown). The origin of this splitting is presently not understood and is only observed for this mode.

4.2. Enhanced Low-Frequency Region, Figure 4. An enlarged view of the region 1280−1480 cm^{-1} is seen in Figure

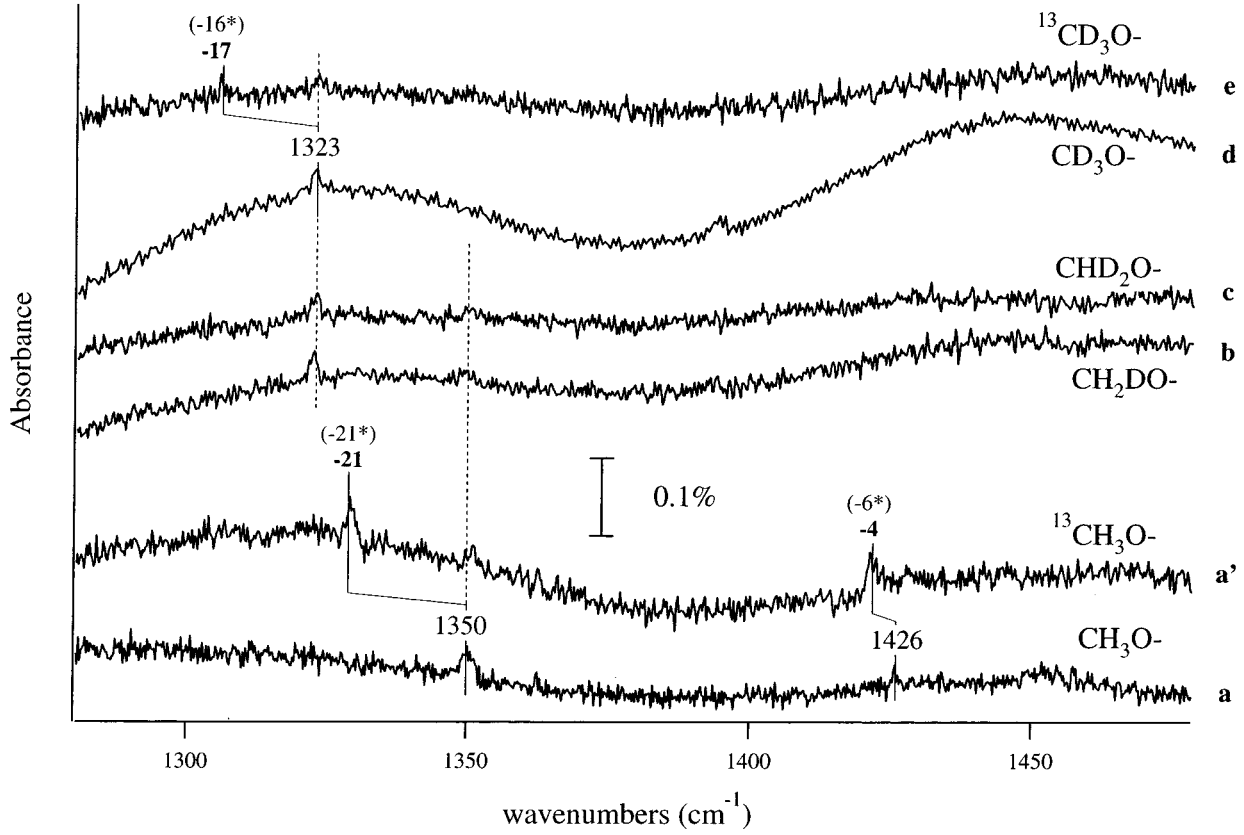

Figure 4. Infrared absorption spectra of (a) CH_3O-, (a′) $^{13}CH_3O-$, (b) CHD_2O-, (c) CH_2DO-, (d) CD_3O-, and (e) $^{13}CD_3O-$ adsorbed on Cu(100).

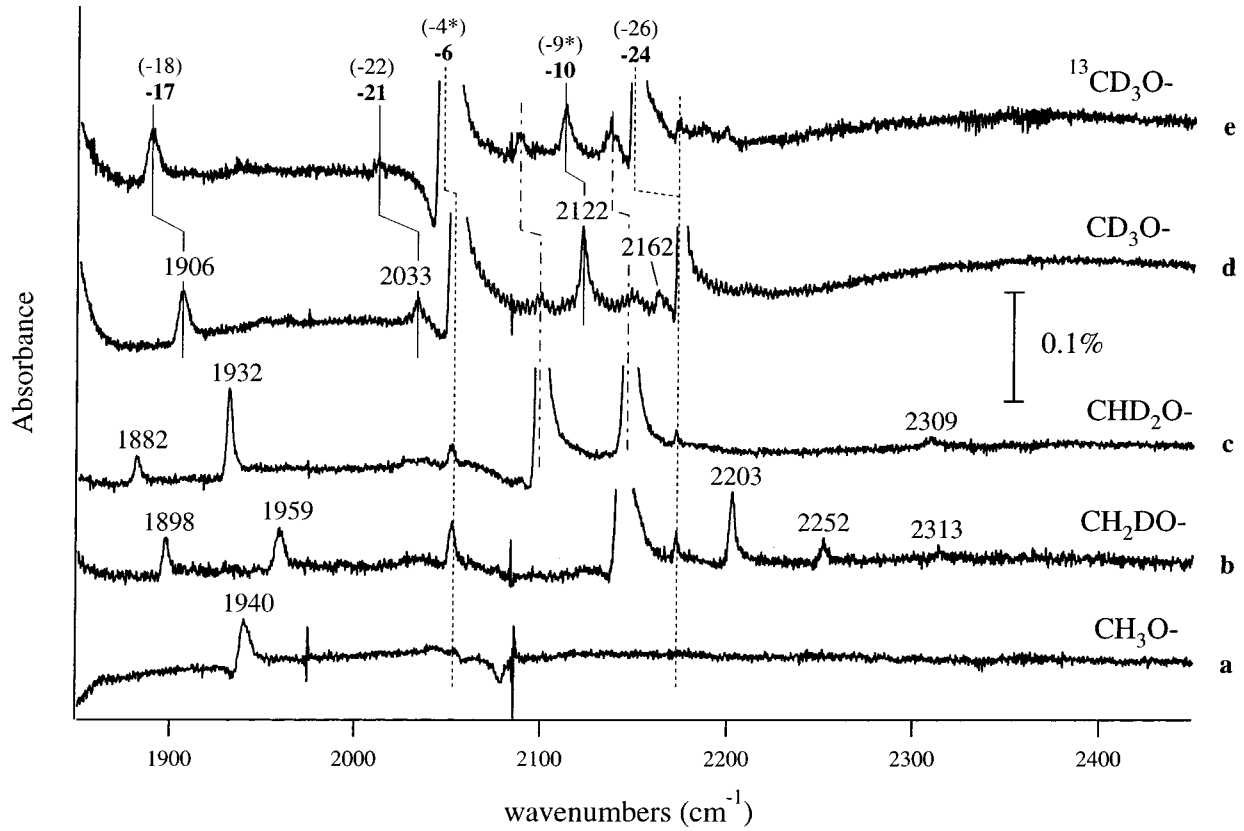

Figure 5. Infrared absorption spectra of (a) CH_3O-, (b) CHD_2O-, (c) CH_2DO-, (d) CD_3O-, and (e) $^{13}CD_3O-$ adsorbed on Cu(100). Dotted and dash/dotted lines indicate isotopic contamination.

4a−e, which is the only region between 600 and 1700 cm^{-1} that contained observable peaks with a peak height <0.1%. The weak mode at 1426 cm^{-1} for CH_3O- is assigned as the symmetric stretch $\delta_s(CH_3)$. The calculated isotopic shift of ∼6 cm^{-1} is again in good agreement with the experimental shift of ∼4 cm^{-1}. The other peaks, observed between 1300 and 1350

TABLE 6: Identification of Frustrated Translations and Rotations (Bold Entries)

mode	symmetry	calcd frequency CH_3O-Cu_5 (cm^{-1})	CH_3O to CD_3O shift (cm^{-1})	^{13}C isotopic shift (cm^{-1})	reduced mass from Gaussian output (amu)	mode assignment
1	**A″**	**−104**	**1**	**0.5**	**11.7**	**FT$_{xy}$**
2	A′	−80	0	0.2	26.0	
3	**A″**	**57**	**−17**	**0.0**	**1.0**	**τ(OCH$_3$)**
4	**A′**	**71**	**−3**	**−0.8**	**8.4**	**FT$_{xy}$**
5	A′	83	0	−0.1	53.0	
6	A″	87	0	0.0	50.7	
7	A′	93	−1	−0.3	18.5	
8	A′	112	−1	−0.3	23.5	
9	**A″**	**125**	**−13**	**−1.4**	**4.2**	**FR**
10	A′	132	−1	−0.3	44.9	
11	A″	132	−1	−0.2	10.5	
12	A″	136	0	0.0	34.3	
13	**A′**	**154**	**−11**	**−1.3**	**4.4**	**FR**
14	A′	174	0	0.0	53.2	
15	**A′**	**271**	**−9**	**−2.4**	**8.2**	**FT$_z$**

TABLE 7: Binary Combinations in the Region 1800−3300 cm^{-1} [a]

exptl mode frequency (cm^{-1})	calcd mode frequency (cm^{-1})	exptl isotopic shift (cm^{-1})	calcd isotopic shift (cm^{-1})	mode assignment
		CH_3O-		
1940	1996			2ν(CO)
2881	2852			$2\delta_s(CH_3)$
2919	2976*			$2\delta_{as}(CH_3)$*
		CH_2DO-		
1898	1916			ν(CO) + δ(OCD)
1959	2016			2ν(CO)
2203	2181*			$2\rho(CH_2)$*
2252	2257*			δ(OCD) + w(CH_2)*
2313	2357*			ν(CO) + w(CH_2)*
2649	2700*			2w(CH_2)*
2856	2957*			2sc(CH_2)*
		CHD_2O-		
1882	1956			w(CD_2) + ν(CO)
1932	2014			2ν(CO)
2146	2134			2sc(CD_2)
2309	2340*			ν(CO) + δ(OCH)*
2583	2642*			2δ(OCH)*
2953	3015*			tw(CD_2)* + $\nu_{as}(CD_2)$*
		CD_3O-		
1906	1942	−17	−18	2ν(CO)
2033	2057	−21	−22	ν(CO) + $\delta_s(CD_3)$
2122	2162*	−10	−10*	$2\delta_{as}(CD_3)$*
2173	2172	−24	−26	$2\delta_s(CD_3)$
3012	3024	−16	−16	ν(CO) + $\nu_s(CD_3)$

[a] Modes have been consistently named after the first mode column in Tables 2−5. Asterisks indicate ab initio values and modes.

cm^{-1}, are associated with trace amounts of formate and assigned to the ν_s(COO) mode in formate. An identification of this species will be given elsewhere, together with calculations.[24] The isotopic shifts based on calculations of the formate species are indicated inside parentheses in the spectra, Figure 4. The vibrational shifts are clearly consistent with formation of formate. Formate formation from methanol and atomic oxygen on, for example, Cu(110) is well-documented.[25]

4.3. Enhanced High-Frequency Region, Figures 5 and 6. The spectra shown in Figures 5a−e and 6a−e cover the frequency region 1850−3200 cm^{-1}. The absorbance scale is enhanced by approximately 1 order of magnitude as compared to the overview spectra in Figure 3a−e. In Figure 7a−d, the graphs show all experimentally observed absorption lines in the spectral region 1800−3200 cm^{-1} as bold lines. All possible binary modes determined from fundamentals are also included as thin lines. These modes are determined from experimental fundamentals when available and from calculation, if experimentally inaccessible. Frequencies based on calculated modes are indicated by a star (*). Fundamentals and overtones are represented by long lines and combination bands by short lines. Binary combinations of A′(A_1 for CH_3O- and CD_3O-) fundamentals are represented by solid lines, and combinations of A″(E for CH_3O- and CD_3O-) fundamentals are represented by dashed lines. An effective C_{3v} symmetry has been assumed for CH_3O- and CD_3O-, which greatly reduces the number of totally symmetric binary combinations. This is done because all spectral features can be accounted for with C_{3v} symmetry and because the calculations show a very small (<4 cm^{-1}) splitting of the degeneracy for the modes involved. For the sake of clarity, isotopic contamination peaks are not included in Figure 7a−d′. In the assignment of the binary overtone and combination modes, we assume a negative anharmonicity as is generally observed for binary modes. To the best of our knowledge, only one exception to a negative value has been reported in the literature for a surface adsorbate.[26]

All binary overtone and combination modes assigned are summarized in Table 7. Most of the assignments are rather straightforward to do because there is in general only one binary mode determined from experimental or calculated values of fundamentals that matches the frequency of the experimentally observed absorption line.

We will now discuss all assignments for the species CH_3O-, CH_2DO-, CHD_2O-, and CD_3O- starting at low wavenumbers. The mode at 1940 cm^{-1} for CH_3O- in Figure 5a is assigned to the 2 × ν(CO) mode. From the "singleton" frequency at 986 cm^{-1} of CH_3O- found in $^{13}CH_3O-$, Figure 2a, the two-phonon bandwidth can be estimated. Because of the anharmonicity of the mode, its overtone is below the bottom of the two-phonon band at 1972 cm^{-1} (2 × 998 − 2 × (998 − 986) = 1972) of the ν(CO) mode. The assignments are summarized in Table 7 and Figure 7a.

The assignment of the two modes in CH_2DO- (Figure 5b and 7b) at 1898 and 1959 cm^{-1} to ν(CO) + δ(OCD) and 2 × ν(CO), respectively, are made with two points in mind. First, the intensity of the ν(CO) mode compared to the δ(OCD) suggests that ν(CO) is involved in both modes because there are no fundamental modes in this region from which intensities could be transferred. Second, the anharmonicity of the CO stretch is normally such that its overtones lie lower than two times the fundamental (see, e.g., ref 27), even though the opposite has been found for a combination band.[26] The two lines at 2203 and 2252 cm^{-1} (Figure 5b and 7b) were assigned to 2 × $\rho(CH_2)$ and δ(OCD) + w(CH_2), respectively, because there were no other modes in the vicinity, see Figure 7b. For the line

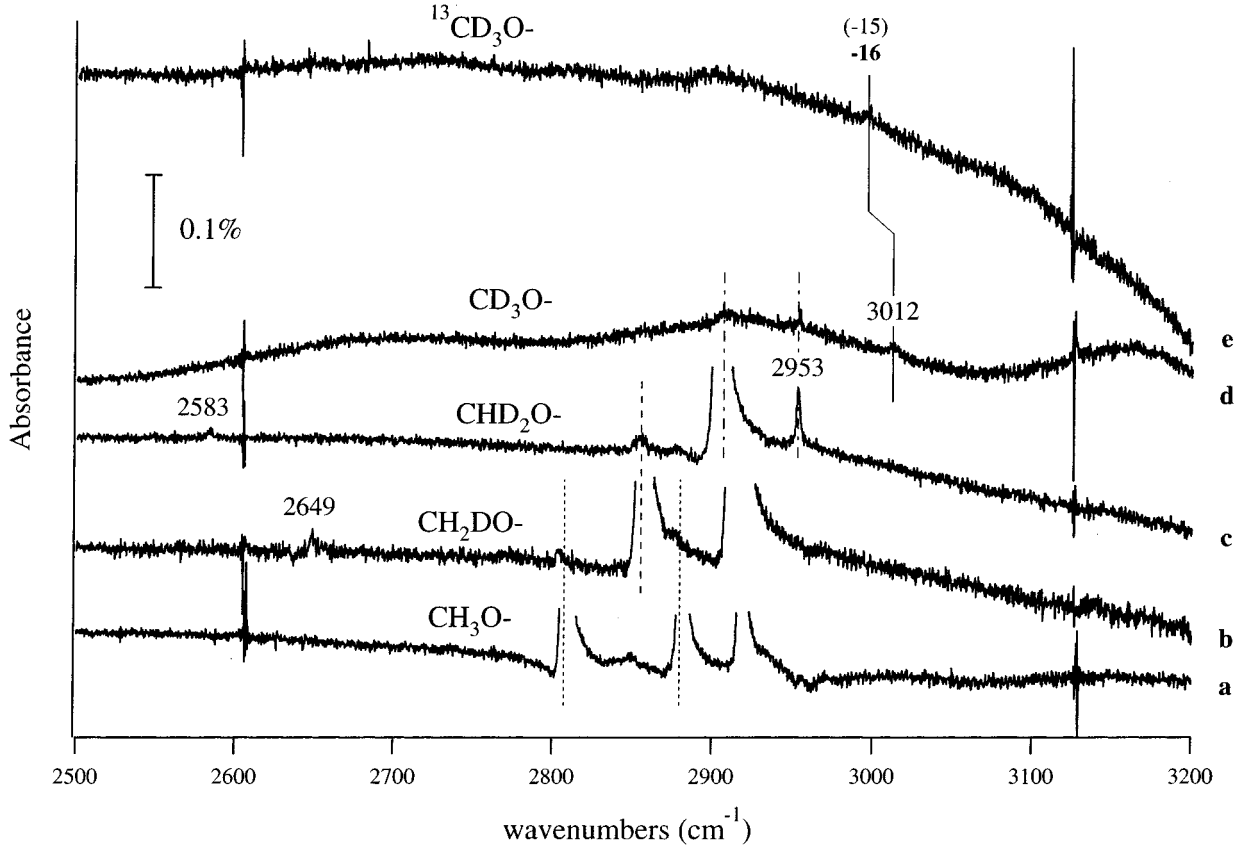

Figure 6. Infrared absorption spectra of (a) CH_3O-, (b) CHD_2O-, (c) CH_2DO-, (d) CD_3O-, and (e) $^{13}CD_3O-$ adsorbed on Cu(100). Dotted and dash/dotted lines indicate isotopic contamination.

observed at 2313 cm^{-1}, Figure 5b, the closest combination $\nu(CO) + w(CH_2)$ was chosen, see Figure 7b. The line at 2649 cm^{-1}, Figure 6b, was assigned as $2 \times w(CH_2)$ consistent with a negative anharmonicity, Figure 7b′.

The two lines at 1882 and 1932 cm^{-1} in CHD_2O^-, Figure 5c, are assigned as $w(CD_2) + \nu(CO)$ and $2 \times \nu(CO)$, respectively, in analogy with CH_2DO-. We favor this assignment based on the observed high intensity of the mode, as opposed to $2 \times w(CD_2)$, the closest mode in Figure 7d, because it includes $\nu(CO)$, which ought to make its intensity higher. Also the observed weak intensity of $2 \times w(CH_2)$ at 2649 cm^{-1}, Figure 6b, is consistent with this assignment and analogous to CH_2DO-. The line at 2309 cm^{-1}, Figure 5c, is assigned as $\nu(CO) + \delta(OCH)$ being the closest mode based on the fundamentals, Figure 7b. The weak feature at 2583 cm^{-1}, Figure 6c, we assign to $2 \times \delta(OCH)$, the only mode close enough (<100 cm^{-1} away), Figure 7c′. The line at 2953 cm^{-1}, Figure 6c, is assigned as $tw(CD_2) + \nu_{as}(CD_2)$, again being the closest mode, Figure 7c′. The next closest mode is ~100 cm^{-1} above, which requires a larger anharmonicity than that observed for any other binary mode observed in the present system. Serrallach and co-workers[28] found in their argon matrix IR spectrum of methanol a feature in this region, which they assigned as the ternary combination $2 \times \nu(CO) + tw(CD_2)$. The fact that the bandwidth is narrower than $2 \times \nu(CO)$, Figure 5c, makes this an unlikely assignment, however.

All modes for the fully deuterated methoxy, CD_3O- and $^{13}CD_3O-$, Figures 5d,e and 7d,d′, have been assigned by virtue of ^{13}C isotopic shifts, Table 7. As previously, the experimental shifts of the fundamentals have been used whenever available. The agreement between calculated and experimental shifts is excellent, Table 7. Together with the experimentally determined combination band shifts, the assignments are unambiguous and prove that the three peaks in the C−D stretch region at 2053, 2122, and 2173 cm^{-1} in CD_3O- are due to Fermi resonances between the symmetric $\nu(CD_3)$ mode and the symmetric and asymmetric $\delta(CD_3)$ modes, in analogy to CH_3O-. Finally, the weak absorption line observed at 3012 cm^{-1} is assigned to the $\nu(CO) + \nu_{as}(CD_3)$ binary combination mode.

A problem that has to be dealt with when looking at low-intensity peaks is how to distinguish impurities from combination bands of the isotope studied. Particularly when dealing with isotopically labeled compounds, the "contamination" from other isotopes can sometimes be as high as 10−20%, and the atomic purity is 98% D in CH_2DO- and CHD_2O- and 99% D in CD_3O-. The major part of the contaminations will therefore be other isotopomers, and intense modes from these isotopes are expected to be observed. Consistently, it is clear by inspection of Figure 5a−e that trace amounts of CD_3O- is present in all isotopomers but CH_3O-. Both the fundamental $\nu_s(CD_3)$ mode at 2053 cm^{-1} and the overtone $2 \times \delta_s(CD_3)$ mode at 2173 cm^{-1} are present for these isotopomers, as indicated by dotted lines in Figure 5a−e. The presence of CHD_2O- in $^{12}CD_3O-$ and $^{13}CD_3O-$ is also apparent in Figure 5 as indicated by the dot−dashed lines at 2099 and 2146 cm^{-1} corresponding to the $\nu_s(CD_2)$ and $2 \times sc(CD_2)$ modes, respectively. Again these assignments are further corroborated by ^{13}C-induced shifts, Figure 5e.

5. Discussion

In a recent study by M. Trenary and co-workers[12] (MT), an empirical force field was derived from five different isotopomers of methoxy adsorbed on Cu(100) exhibiting C_{3v} symmetry. From this force field, the vibrational spectra of two different C_s

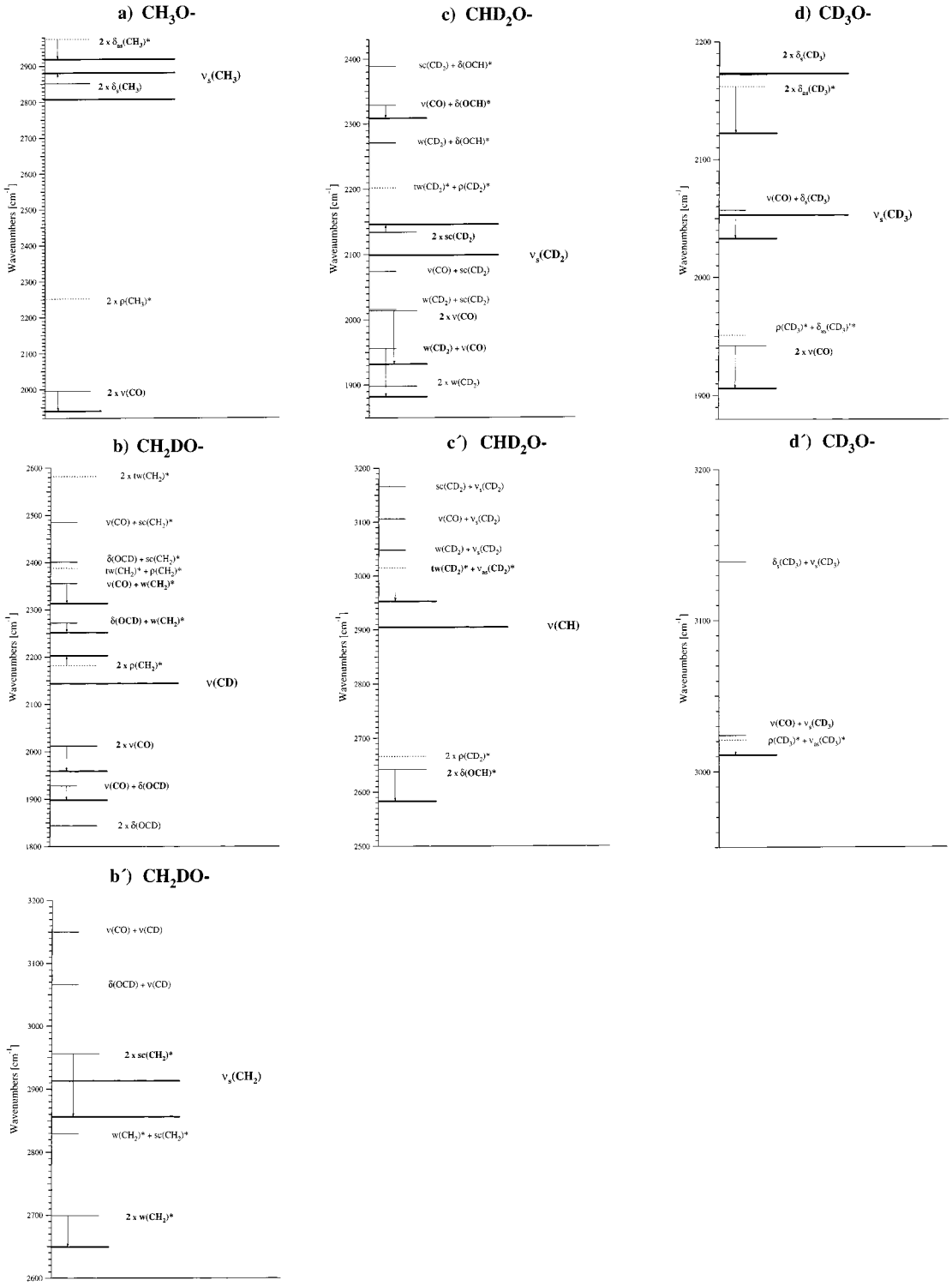

Figure 7. Graphic representation in the 2000−3200 cm^{-1} region of experimentally observed modes showed as bold lines, for which the length of the lines is an indication of intensity. Narrow lines correspond to binary modes determined from experimental fundamentals, full lines are binary combinations of A′ (A_1) fundamentals, whereas dotted lines are binary combinations of A″ (E) fundamentals. Modes marked with ∗ are calculated values. The isotopomer and wavenumber region is as follows: (a) CH_3O^-, 1920−2980 cm^{-1}; (b) CH_2DO- 1800−2600 cm^{-1}; (b′) CH_2DO-, 2600−3200 cm^{-1}; (c) CHD_2O-, 1850−2450 cm^{-1}; (c′) CHD_2O-, 2500−3200 cm^{-1}; (d) CD_3O-, 1880−2200 cm^{-1}; (d′) CD_3O-, 2900−3200 cm^{-1}.

symmetric isotopomers were successfully determined. The assignments made by MT are essentially the same as ours. The most striking difference is that we identify and assign an additional seven weak IR lines, which makes the assignment of the more intense lines more conclusive.

In addition, ab initio calculations of five C_{3v} symmetric methoxy−Cu complexes was also performed in the study by MT. It was shown that this complex gave a description of the vibrational spectra of methoxy adsorbed on Cu(100) inferior to the empiric force field. Most disturbing was the inability of the ab initio calculations to correctly determine the experimentally observed order of the ν(CO) and $\delta_s(CD_3)$ modes in the CD_3O- species. This is, however, not too surprising because the one copper atom representation of the surface in this case inad-

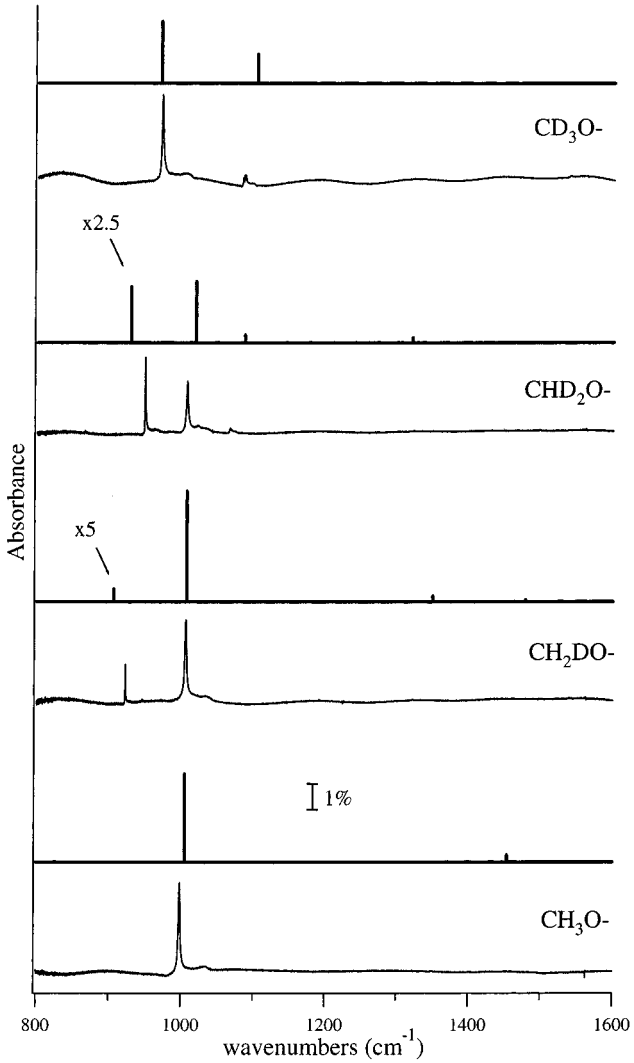

Figure 8. Comparison of experimental and calculated vibrational spectra. Intensities are normalized with respect to the CH_3O- spectrum. The small arrows in the CHD_2O- and CH_2DO- spectra indicate lines for which the calculated intensities also are compensated for narrow line widths because the simulated spectra are represented by height only.

equately describes the surface adsorbate interaction. We have previously used one molybdenum atom to represent the Mo(110) surface and shown that the intramolecular modes of adsorbed methoxy are well-described.[18] For the one-Mo-atom description, however, the C_{3v} structure (180° O−C−Mo angle) is a minimum, whereas the one-Cu-atom description with enforced C_{3v} symmetry gives two imaginary frequencies of E symmetry. We have recently showed[20] that a five copper atom cluster adequately models the alkoxy−Cu(100) interaction. The single copper atom representation leads to an overestimation of the ν(CO) mode frequency, whereas the $\delta_s(CD_3)$ mode is much less influenced by the coordination to the metal. As a consequence, the coupling between the two modes will be overestimated. This is most probably causing the reversed frequency order observed for these modes in the one copper atom ab initio calculations upon deuteration. As seen in Table 5, our five atom copper cluster representation of the surface adequately reproduces the experimentally observed order. Accordingly, the intensities of the fundamental modes in the 800−1600 cm^{-1} region are also correctly reproduced by this representation of the Cu(100) surface, Figure 8.

In contrast to MT, we can observe both the $\delta_s(CH_3)$ mode and the $2 \times \nu$(CO) mode for the same preparation procedure even though our coverage, ∼0.3 ML, is lower than what they studied, ∼0.5 ML. The advantage of using a lower coverage is that it gives a more homogeneous overlayer as is most apparent in the CH stretch region where inhomogeneous broadening is observed at ∼0.5 ML.[12]

Our study also shows that the assignments of the C−D stretch region of deuterated methoxy adsorbed on Cu(111)[3] and Ag(111)[2] probably are incorrect. On Ag(111), the line at 2123 cm^{-1} was assigned to the ν(CO) + $\delta_s(CD_3)$ mode and the line observed at 2185 cm^{-1} to a doublet consisting of $2 \times \delta_s(CD_3)$ and $2 \times \delta_{as}(CD_3)$. The combinations of ^{13}C labeling and calculations allow us to conclusively assign the line at 2123 cm^{-1} to the $2 \times \delta_{as}(CD_3)$ overtone and the line at 2173 cm^{-1} to $2 \times \delta_s(CD_3)$, Figure 7d and Table 7. The strong similarity between the absorption line positions makes us quite confident that this assignment is the correct one for Ag(111)[2] and Cu(111)[3] as well. The energy of the line observed at 2123 cm^{-1} on Ag(111), if assigned as the ν(CO) + $\delta_s(CD_3)$ (1105 + 1008 = 2113), also requires that it is blue-shifted by FR with the $\nu_s(CD_3)$ mode. As discussed more below, FRs between fundamental methyl stretch modes and binary combination modes are much weaker than FRs between methyl stretch modes and overtone modes.

It is well-known that the scaling of CH bend and stretch modes are somewhat different for HF force fields.[29] If the same scale factor is used for both modes, the bending modes will be slightly overestimated. The difference between the calculated value and the experimental value of the $\delta_s(CH_3)$ mode for CH_3O- (exptl 1426 vs calcd 1446 cm^{-1}) is 20 cm^{-1}. If we assume that the difference is systematic in nature and apply it to all CH deformation modes, this would further improve the agreement between experiment and calculations as almost all calculated CH deformation overtones are too high. All CO stretch overtones and combination bands are also too high, but this is due to the dipole coupling of the fundamental and the nonnegligible anharmonicity. These two observations explain all of the significant discrepancies between experiment and calculation with the notable exception of (tw(CD_2) + $\nu_{as}(CD_2)$), which is calculated to be 62 cm^{-1} above the experimental value (see also discussion below).

We will now discuss some similarities between the spectra of the various isotopomers and draw some qualitative conclusions about the anharmonic coupling in the system. For all isotopomers the overtone of the ν(CO) mode is observed. Furthermore, for the deuterated species, the binary combinations of the ν(CO) mode and the first totally symmetric mode below it are observed. The modes are δ(OCD) for CH_2DO- and w(CD_2) for CHD_2O-. For these modes, it is probably the high intensity of the fundamentals and a substantial anharmonicity that give the intensity of the binary combinations. For CHD_2O-, there is also a substantial coupling between the two fundamental modes, ν(CO) and w(CD_2), Table 4. These binary overtones and combinations modes are "true" binary modes in the sense that the intensity and the energy of them are not enhanced or perturbed by Fermi resonances coupling to any fundamental mode.

All totally symmetric fundamental C−H stretches and C−D stretches are observed, with the exception of the A′ modes that in C_{3v} symmetry would be of E symmetry, Table 1. These observations are consistent with an effective C_{3v} symmetry of the CH_3O- and CD_3O- species, in agreement with previous experimental results.[14,12]

The coupling of the C−H and C−D stretch modes to the various bend overtones is very similar for all isotopomers. With

only a few exceptions ($2 \times$ tw(CH_2) and $2 \times$ w(CD_2)), all binary overtones of CH bends and CD bends are observed. It follows from the weak intensity of the fundamental of these modes that the overtones of them have to be in Fermi resonance with the fundamental symmetric C−H stretch and symmetric C−D stretch, respectively. The strength of the coupling and hence the intensity of the overtone depend on the energy difference of the unperturbed modes (for a two-state problem it is inversely proportional to the energy difference, see, for example, ref 30) and the symmetry of the fundamental bend mode. The observed coupling is, however, stronger for the overtones of the bend modes the fundamentals of which are totally symmetric, that is, have A′ symmetry (or A_1 symmetry in the C_{3v} point group) irrespective of the energy difference between the modes. Presently, we do not have a physical explanation for this behavior.

Coupling between C−H stretch and binary modes consisting mostly of CD movement is observed to be much weaker than coupling between modes consisting of motion of the same atoms, such as the coupling between, for example, $\nu(CH_2)$ and $2 \times$ sc(CH_2). This is the case even though the energy separation between the binary mode and the corresponding fundamental is comparable to the stretch/$2 \times$ bend FR for the "same atoms". This phenomenon is also consistently observed for the C−D stretch with respect to the binary modes consisting of CH bend movement. The two examples found are the $2 \times \rho(CH_2)$ at 2203 cm^{-1} in FR with fundamental ν(C−D) mode for CH_2DO- and the tw(CD_2) + $\nu_{as}(CD_2)$ mode at 2953 cm^{-1} in FR with fundamental ν(C−H) for CHD_2O-. The energy difference between the fundamental ν(C−D) mode and the $2 \times \rho(CH_2)$ mode is 59 cm^{-1} and essentially the same as the energy difference (57 cm^{-1}) between the fundamental $\nu(CH_2)$ mode and the $2 \times$ sc(CH_2) mode, Figure 3b. Similarly, for CHD_2O-, the energy difference between the combination modes tw(CD_2) + $\nu_{as}(CD_2)$ and the fundamental ν(CH) mode is 48 cm^{-1}, whereas the corresponding difference between the $\nu(CD_2)$ mode and the $2 \times$ sc(CD_2) mode is again essentially the same, 47 cm^{-1}, Figure 3c. The intensity difference, however, between the "same atoms" and "different atoms" Fermi resonances is at least an order of magnitude weaker for the "different atom" resonance, Figure 3b,c. The physical origin for this phenomenon is not known.

The coupling of the fundamental C−H and C−D stretches to binary combination bands consisting of different fundamentals is, in general, much weaker than the coupling to overtones. All such observed combinations have a component of either the intense ν(CO) or δ(OCH) fundamental mode. This makes us believe that these binary combinations are "true" combination modes. That is, these modes are probably not influenced by FR coupling to any fundamental mode. The (tw(CD_2) + $\nu_{as}(CD_2)$) mode observed for CHD_2O- is again a notable exception, as discussed above.

The assignment of the line at 2953 cm^{-1} to the tw(CD_2) + $\nu_{as}(CD_2)$ mode of CHD_2O- is more uncertain than any other assignment because its calculated frequency is far from the experimental value (62 cm^{-1}) and it is the only combination band observed without an intense fundamental component. At the time of writing, we have no explanation for this anomaly. It is, however, the mode closest in frequency to the observed line, Figure 7.

6. Conclusions

In conclusion, we have assigned the vibrational spectra of various methoxy isotopomers adsorbed on a Cu(100) surface in great detail. The assignments are based on ab initio calculations of the vibrational mode frequencies of a methoxy−Cu_5 complex and all of the investigated methoxy isotopomers. By combining different detectors and optical filters, we observe many, previously undetected, weak spectral features, which we can assign as various binary overtone and combination modes. The calculations were necessary for the assignments of several of the binary modes because one or both contributing fundamental modes were not experimentally observed but had to be calculated. On the basis of these binary modes, conclusions on the intramolecular anharmonic coupling in the adsorbate can be drawn. The strength of our expanded ab initio calculation approach from the single metal atom representation of the surface is also clearly demonstrated. The major challenge that now remains is to include the Fermi resonance coupling on an ab initio level as well.

Acknowledgment. We thank and acknowledge financial support from the Swedish Natural Science Research Council.

References and Notes

(1) Ryberg, R. *Phys. Rev. B* **1985**, *31*, 2545−7.
(2) Sim, W. S.; Gardner, P.; King, D. A. *J. Phys. Chem.* **1995**, *99*, 16002−16010.
(3) Chesters, M. A.; McCash, E. M. *Spectrochim. Acta* **1987**, *43A*, 1625.
(4) Uvdal, P.; Weldon, M. K.; Friend, C. M. *Phys. Rev. B (Rapid Commun.)* **1994**, *50*, 12258.
(5) Dastoor, H. E.; Gardner, P.; King, D. A. *Chem. Phys. Lett.* **1993**, *209*, 493−498.
(6) Ḥuberty, J. S.; Madix, R. J. *Surf. Sci.* **1996**, *360*, 144.
(7) Ásmundsson, R.; Uvdal, P. Unpublished work.
(8) Dastoor, H. E.; Gardner, P.; King, D. A. *Chem. Phys. Lett.* **1993**, *209*, 493.
(9) Zenobi, R.; Xu, J.; Yates, J. T.; Persson, B. N. J.; Volokitin, A. I. *Chem. Phys. Lett.* **1993**, *208*, 414.
(10) Jayasooriya, U. A.; Anson, C. E.; Al-Jowder, O.; Alfonso, G. D.; Stanghellini, P. L.; Rossetti, R. *Surf. Sci.* **1993**, *294*, 131.
(11) Camplin, J. P.; McCash, E. M. *Surf. Sci.* **1996**, *360*, 229−241.
(12) Mudalige, K.; Warren, S.; Trenary, M. *J. Phys. Chem. B* **2000**, *104*, 2448.
(13) Mudalige, K.; Trenary, M. *J. Phys. Chem. B* **2001**, *105*, 3823.
(14) Ásmundsson, R.; Uvdal, P. *J. Chem. Phys.* **2000**, *112*, 366.
(15) Giguere, J.; Overned, J. *Spectrochim. Acta* **1976**, *32A*, 241.
(16) Ryberg, R. *J. Chem. Phys.* **1985**, *82*, 567−73.
(17) Frisch, M. J.; Trucks, G. W.; Schlegel, H. B.; Scuseria, G. E.; Robb, M. A.; Cheeseman, J. R.; Zakrzewski, V. G.; Montgomery, J. A., Jr.; Stratmann, R. E.; Burant, J. C.; Dapprich, S.; Millam, J. M.; Daniels, A. D.; Kudin, K. N.; Strain, M. C.; Farkas, O.; Tomasi, J.; Barone, V.; Cossi, M.; Cammi, R.; Mennucci, B.; Pomelli, C.; Adamo, C.; Clifford, S.; Ochterski, J.; Petersson, G. A.; Ayala, P. Y.; Cui, Q.; Morokuma, K.; Malick, D. K.; Rabuck, A. D.; Raghavachari, K.; Foresman, J. B.; Cioslowski, J.; Ortiz, J. V.; Stefanov, B. B.; Liu, G.; Liashenko, A.; Piskorz, P.; Komaromi, I.; Gomperts, R.; Martin, R. L.; Fox, D. J.; Keith, T.; Al-Laham, M. A.; Peng, C. Y.; Nanayakkara, A.; Gonzalez, C.; Challacombe, M.; Gill, P. M. W.; Johnson, B. G.; Chen, W.; Wong, M. W.; Andres, J. L.; Head-Gordon, M.; Replogle, E. S.; Pople, J. A. *Gaussian 98*; revision A.9; Gaussian, Inc.: Pittsburgh, PA, 1998.
(18) Uvdal, P.; MacKerell, A. D., Jr. *Surf. Sci.* **1997**, *393*, 141.
(19) Carvalho, A. V. d.; Asensio, M. C.; Woodruff, P. D. *Surf. Sci.* **1992**, *271*, 381.
(20) Andersson, M. P.; Uvdal, P., manuscript in preparation.
(21) Kuczera, K.; Wiorkiewicz-Kuczera, J.; Karplus, M. *MOLVIB* program is a module in *CHARMM*, Copyright 1984−2001; President and Fellows of Harvard College: Cambridge, MA, 1998. All Rights Reserved.
(22) Aberhart, J. Private communication.
(23) Head, J. D.; Shi, Y. *Int. J. Quantum Chem.* **1999**, *75*, 815.
(24) Andersson, M. P.; Uvdal, P., manuscript in preparation.
(25) Silva, S. L.; Patel, A. A.; Pha, T. M.; Leibsle, F. M. *Surf. Sci.* **1999**, *441*, 351.
(26) Jakob, P.; Persson, B. N. J. *J. Chem. Phys.* **1998**, *109*, 8641.
(27) Uvdal, P.; Weldon, M. K.; Friend, C. M. *Phys. Rev. B* **1996**, *53*, 5007.
(28) Serrallach, A.; Meyer, R.; Günthard, H. H. *J. Mol. Spectrosc.* **1974**, *52*, 94.
(29) Florián, J.; Johnson, B. G. *J. Phys. Chem.* **1994**, *98*, 3681.
(30) Herzberg, G. *Infrared and Raman Spectra of Polyatomic Molecules*; Van Nostrand Reinhold Company, Inc.: New York, 1945; Vol. II.